

Research Article

CNC Milling and CO₂ Laser Engraving of Mixing Microchannels in Microfluidic Devices

Zachary Ngo*, Catherine Joy Cancino, Jedrek Carl Dy, Brent Schyler Uy, Richard Josiah Tan Ai and Ronnie Concepcion II

Department of Manufacturing Engineering and Management, De La Salle University Manila, Manila, Philippines

* Corresponding author. E-mail: zachary_ngo@dlsu.edu.ph

DOI: 10.14416/j.asep.2025.10.001

Received: 13 May 2025; Revised: 15 July 2025; Accepted: 22 August 2025; Published online: 1 October 2025

© 2025 King Mongkut's University of Technology North Bangkok. All Rights Reserved.

Abstract

Microfluidic devices play a crucial role in biomedical research, chemical analysis, and diagnostics, with fabrication optimization striking a balance between precision, efficiency, and cost-effectiveness. Currently, there is a need to determine the most suitable fabrication technique for accuracy, efficiency, and material compatibility. This study compared computer numerical control (CNC) milling machines and CO₂ laser engraving machines by investigating their strengths and weaknesses as microfluidic device fabrication techniques. Microfluidic devices were designed with mixing microchannels of 1.0 mm width and depth using Autodesk Fusion. Autodesk Fusion was further utilized to configure the drilling and tracing processes of the milling operation, while RDWorks V8 was utilized for laser setup. Three materials with varying chemical resistances, optical properties, mechanical strengths, fabrication feasibility, and cost were selected. Polymethyl methacrylate (PMMA) is cost-effective and optically transparent, polycarbonate offers mechanical robustness and ease of processing, and borosilicate glass possesses outstanding chemical resistance, mechanical strengths, and optical properties. Testing was accomplished through microscopic imaging and colorimetric analysis through a manual pump with a constant downward mass of 461 g. Microchannel precision and fluid flow characteristics determined the effectiveness of each fabrication technique. Based on the food coloring-water mixture mixing capabilities of the manufactured chips, CNC milling presents a significant advantage over laser engraving in channel fabrication due to its ability to produce more consistent microchannels and smoother surfaces. In turn, this results in enhanced fluid flow and mixing efficiency. Polymethyl methacrylate (PMMA) displays the most ideal and cost-effective results through microscopic visualizations and color analysis, with a CNC-milled device being accomplished in 5 min with an overall setup time of approximately 20 min. Thus, making the combination an excellent choice for mass production. This study highlights the significance of utilizing the optimal fabrication technique for microfluidic devices to strike a balance between precision, efficiency, and cost-effectiveness and yield a device that is viable for a broad range of applications from biomedical to chemical fields.

Keywords: Lab-on-a-Chip, Microchannel fabrication, Microfluidic, Micromachining, Precision engineering

1 Introduction

Microfluidic systems are versatile, small-scale devices with detailed channels designed to enable the controlled movement of liquid samples via forces such as electrokinetic, capillary, or vacuum [1], [2]. Scientific and industrial fields have benefited from the introduction of microfluidic technologies by enabling precise fluid control and manipulation. Microfluidic devices are utilized in various fields, ranging from

biomedical diagnostics to lab-on-a-chip technology, where they enhance reaction efficiency, ensure sample homogeneity, and improve overall device performance. The design of efficient mixing microchannels is a crucial element of these chips, as rapid and uniform mixing is facilitated. In comparison to conventional methods, the fabrication methods of microfluidic chips face hurdles in terms of production costs, scalability, and design constraints.

From intricate channels to dynamic flows, the realm of microfluidic devices encapsulates prodigious possibilities. Microfluidic devices, which function at the microscale level and regulate the flow of small volumes of fluids, have gained an abundance of interest since the 1990s [3]. Their development was driven by miniaturization and fabrication advancements in the electronics industry, with early contributions from various fields shaping microfluidics into a standalone science. Emerging in the 1980s and 1990s, technology has since evolved into a foundational tool across numerous applications [4].

Current small-scale medical device fabrication processes are often hindered by high costs, lengthy turnaround times, and limited accessibility to specialized equipment. Techniques such as soft lithography, photolithography, and injection molding typically require cleanroom environments and costly infrastructure, making them impractical for rapid prototyping or low-volume production. These limitations underscore the growing need for more efficient, scalable, and cost-effective fabrication approaches. To address these challenges, Kruk and Wippold developed PRIMDEX, a low-cost, open-source microfluidic fabrication platform that enables rapid prototyping using laser engraving and off-the-shelf materials, significantly reducing device iteration time and cost [5]. Yasman *et al.*, introduced a method for directly fabricating microfluidic channels on glass using a CO₂ laser, eliminating the need for molding and complex post-processing while achieving high surface quality and design flexibility [6]. Similarly, Leclerc *et al.*, demonstrated a hybrid approach using CNC micromilling and anisotropic shrinking of stressed polystyrene sheets, enabling consistent, low-cost microfluidic chip production with high reproducibility and resolution without cleanroom facilities [7].

Umpteen processes, both in the field of chemistry and biology, can be automated through the adaptation of microfluidic devices. Not only will productivity be augmented, but repeatability and reproducibility are also heightened [8]. Among the plentiful applications of microfluidic systems, those focusing on handling minute volumes of fluids for medical, biological, and chemical applications are developing at a rapid pace [3]. Lower manufacturing costs, reagent consumption, and analysis times are among the advantages observed through the utilization of these devices, in addition to those of device efficiency and portability [3].

Microfluidic devices employ various advanced techniques to enhance their applications across multiple fields. In diagnostics and healthcare, techniques such as inertial microfluidics, magnetophoresis, and immunolabeling facilitate efficient cell manipulation, enabling low-cost and precise disease detection [9], [10]. For pharmaceutical research, microfluidic chips offer rapid drug screening and analysis within controlled cellular environments, reducing reagent consumption and experimental costs [11]. Additionally, in material synthesis and environmental monitoring, microfluidics is leveraged for nanomaterial fabrication, water purification, and sensor development, enhancing efficiency in contamination detection and food safety monitoring [12], [13]. The precise control of fluid flow at the microscale further allows liquid-liquid extraction processes, optimizing solvent separation techniques with minimal resource usage [14]. Despite these advancements, challenges such as the need for specialized equipment and scalability constraints remain critical considerations in microfluidic technology applications [11].

Numerous advancements are available in the production of microfluidic devices, with each technique offering distinct advantages and considerations based on the requirements needed. Some of these techniques include micro-injection molding, hot embossing, thermoforming, electron-beam or focused ion beam (FIB) machining, casting, milling, lamination, laser cutting, 3D printing, and roll-to-roll (R2R) processing [8]. Recent patents demonstrate the use of magnets for biomarker detection [15], laser-based fabrication for targeted cell manipulation [16], and 3D-printed hydrogel biomaterials for biomedical applications [17], highlighting innovative approaches that enhance microfluidic precision and scalability. These techniques offer high-volume production, nanometer detail transfer, thin and 3D structures, and process size restrictions. In contrast, other techniques offer advantages such as cost, replicability, material compatibility, and process complexity. Scientists and engineers must carefully evaluate these techniques based on minimum feature sizes, surface roughness, aspect ratio, and working size to optimize the fabrication process for specific microfluidic device applications [8].

The two methods that will be utilized in this study, namely laser engraving and computer numeric control (CNC) milling, are amongst the several other methods mentioned in the previous paragraph. For a more in-depth explanation of these two methods, laser

cutting has been a state-of-the-art method in the fabrication of inertial microfluidic devices [18]. It is a rapid manufacturing technique that utilizes laser plotters to engrave the surface of various materials. This approach is advantageous in terms of speed and non-contact processing, therefore making it ideal for fabricating intricate channel designs with smooth surfaces.

On the flip side, CNC milling is another fabrication technique that is widely utilized in the manufacturing industry [19]. The technique is a subtractive manufacturing technique that is used for the rapid prototyping of microfluidic devices, as it involves the selective removal of materials from a sample. With its exceptional accuracy, it is a suitable approach for prototyping and low-volume production. Furthermore, CNC milling provides a wide range of material processing capabilities, as it provides flexibility in device design and material selection.

Several factors come into play, such as the capabilities of laser engraving and CNC milling. These include the accuracy of the design, cost of the chip, product scalability, and material compatibility. The process of CNC milling is advantageous in terms of depth control and fabricating chips that require robust structural integrity. On the other hand, laser engraving is advantageous in terms of rapid prototyping and speed. The previously mentioned fabrication techniques will be investigated through the creation of a mixing microfluidic device, where the process of mixing is a vital component in microfluidic devices, as it determines the result of the succedent phases [3].

Leakage is a common and potentially serious issue in microfluidic devices, impacting both safety and performance. Leakage testing is crucial to ensure reliable device operation. Common methods for detecting leaks include visual inspection, liquid and gas pressure drop tests, and high-temperature testing. Failure Mode and Effects Analysis (FMEA) can be employed to identify and mitigate leakage risks [20]. Beyond leak detection, dye and pH tests can also verify proper substance mixing. For example, food dye has been used to assess micromixer functionality by visually inspecting the output and comparing it to simulations [21]. Similarly, pH testing with colorimetric detection has been used to verify mixing accuracy on microfluidic paper-based platforms by analyzing hue values correlated to pH levels [22].

This study provided a comprehensive review of the feasibility and effectiveness of CNC milling machines and laser engravers for fabricating mixing

microchannels. With the objective of comparing the structural integrity, surface quality, and fluid dynamics of each chip, an optimized fabrication strategy has been proposed to improve microfluidic device performance. The use of borosilicate glass, polymethyl methacrylate (PMMA), and polycarbonate has been investigated to determine which variation offers the best channels. Through three trials with each material variation, the study determined the most cost-effective combination of methods for fabricating optical mixing microchannels. Basic statistical analyses conducted include calculations of the mean, standard deviation, and the coefficient of variation for key performance metrics. These performance metrics include channel dimensions, flow uniformity, and mixing efficiency. Resultant of this is the combination of the most cost-effective methods for fabricating optimal mixing microchannels. With consistent fabrication and testing techniques, reproducibility across multiple devices is attainable.

This research makes the following contributions. Firstly, development of a comparative analysis of CNC milling and CO₂ laser engraving technologies for the fabrication of mixing microchannels in microfluidic devices. This provides insights into balancing the structural integrity, surface quality, and fluid dynamics of each device. Secondly, introduction of an optimal fabrication strategy based on the experiment findings to provide further details into the ideal combination between CNC milling and CO₂ laser engraving. This will yield high-quality microchannels in microfluidic devices. Thirdly, evaluation of borosilicate glass, PMMA, and polycarbonate as potential materials for microfluidic device fabrication. The ideal material will be identified based on the mechanical and fluidic properties. Fourthly, a cost-effective combination for microfluidic device fabrication to facilitate efficient production of high-performance microfluidic devices at lower costs. This study sets the stage for the broader adoption of microfluidics in practical applications.

2 Materials and Methods

A five-step process was used to compare CNC milling and laser engraving for microfluidic device fabrication, as seen in Figure 1. Commencing with design, Autodesk Fusion was used to design the devices according to their respective specifications. Moving on, material selection was done through an analysis of material optical transparency, chemical

resistance, machinability, and cost-effectiveness. Determination of fabrication parameters is then conducted based on the material properties, playing a crucial role in ensuring that chips are manufactured with utmost quality. Before testing, post-processing techniques are conducted to eliminate impurities and ensure that testing is conducted with minimal error.

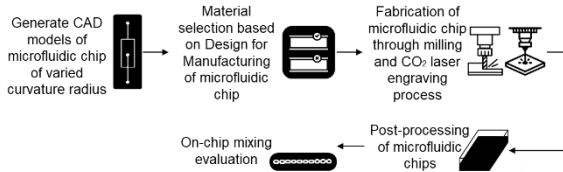


Figure 1: Step-by-step process of comparing CNC milling and laser engraving of mixing microchannels in microfluidic devices.

2.1 Generation of computer-aided design models of a microfluidic chip

The essence of microfluidic device fabrication lies in the intricate process of computer-aided design (CAD) drawing. Drawings were created on an Apple MacBook Pro running an M3 Pro chip, running the CAD software Autodesk Fusion version 2.0.20476. These drawings pave the way for frameworks concerning the succeeding milling and engraving processes, with the sample in Figure 2 presenting the 3-D model of a chip with a 1 mm radius. Microfluidic chips with microchannels of 1 mm width and depth were first crafted. This combination of width and depth was selected despite smaller microchannels ($<300\ \mu\text{m}$) being more suitable due to equipment limitations for resolution and depth control at smaller scales. Nevertheless, the combination of 1mm width and depth provides a respectable baseline for a comparison of the two fabrication techniques. In these microchannels lies the combination of linear and diagonally oriented channels, with the specific lengths allowing for fluid handling in mixing operations. Materialization of the design process included iterative CAD modeling and simulation with the aid of Autodesk Fusion. These iterations encompassed the adjustment of channel curvature and cross-sectional profiles to enhance the mixing of fluids and minimize the possibility of stagnation zones. Attributable to the simulation capabilities of Autodesk Fusion, efficiency, precision, performance assessment, and risk mitigation were augmented. The design was considered optimized once the intended dimensions were successfully attained and fabricated without defects. Considerations

include device manufacturability, structural integrity, and consistency. Subsequently, the files were converted to GCode for CNC milling and RD files for laser engraving.

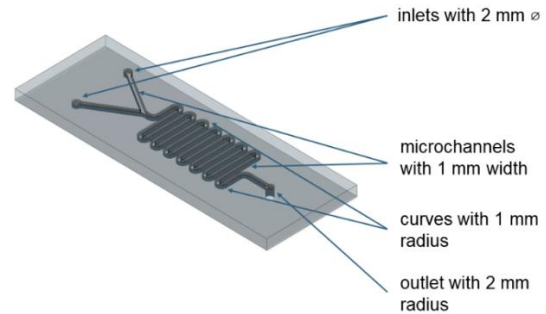


Figure 2: 3-D model of a microfluidic chip with serpentine channels of 1 mm radius.

2.2 Selection of materials

The accomplishment of the CAD drawings paves the path for the subsequent steps of microfluidic device manufacturing. The process commences with material selection, with this study focusing on three materials: borosilicate glass, polymethyl methacrylate (PMMA), and polycarbonate. The choice of materials was meticulously settled upon by considering the manufacturing techniques to be investigated, particularly CNC milling and laser cutting.

Table 1 delves into a comparison of the evaluated materials for the study, with Table 2 presenting a quantitative look into various properties of the three materials selected. Borosilicate glass is the first material selected. It is renowned for its durability despite its cutting challenges and heightened costs. This material is optimal for a broader range of microfluidic applications due to its hardness and susceptibility to heat-affected zones [23]. An excellent alternative to borosilicate glass for microfluidic device applications lies in PMMA. This material presents excellent characteristics for microfluidic device applications due to its low cost, excellent optical transparency, ease of fabrication, and many more [24]. Polycarbonate is the third material to be studied, attributable to its augmented impact resistance, low moisture absorption, and low costs. In addition, this material has a high glass transition temperature and is compatible with mass production through injection molding and hot embossing manufacturing techniques [25]. Due to other factors, such as cost, fabrication challenges, or chemical resistance insufficiencies, the other materials were excluded.

Table 1: Comparison of the various materials evaluated during the process of selecting the materials.

Material	Optical Transparency	Machinability	Chemical Resistance	Cost	Justification for Selection / Exclusion
PMMA	High	Excellent	Moderate	Low	Cost-effective, transparent, easy to machine
Polycarbonate	Moderate	Good	High	Medium	Mechanical strength and chemical resistance
Borosilicate Glass	High	Difficult	Excellent	High	Chemical resistance
Soda Lime Glass	High	Difficult	Low	Low	Less durable and chemical resistant alternative to borosilicate glass
Cyclic Olefin Polymer (COP)	High	Moderate	High	Medium	Less accessible and more expensive than PMMA
Cyclic Olefin Copolymer (COC)	High	Moderate	High	Medium	Similar to COP but less cost-effective than PMMA
Polydimethylsiloxane (PDMS)	High	Easy	Low	Low	Poor chemical resistance and stability

Table 2: Quantitative comparison of the selected materials for microfluidic chip fabrication.

Properties	Material		
	PMMA	Polycarbonate	Borosilicate Glass
Optical Transparency	~92% ^[26]	~86% ^[27]	~88% ^[28]
Surface Roughness	~0.15 μm (CNC Milling) ^[29] / 7 – 1.72 μm (Laser engraving) ^[30]	~0.2 μm (CNC Milling) ^[31]	250 nm (Ductile mode Micro-end Milling) ^[29]
Machinability	Excellent	Good	Difficult
Chemical Resistance	Moderate – incompatible with strong oxidizing agents, strong acids ^[32]	High – incompatible with strong oxidizing agents ^[33]	Excellent – incompatible with strong oxidizing agents ^[34]
Cost	Low	Medium	High
Justification for Selection	Cost-effective, transparent, easy to machine	Mechanical strength and chemical resistance	Chemical resistance

2.3 Experimenting with specific fabrication parameters

The material selection process is followed by fabricating microfluidic chips. As mentioned previously, this study incorporated two machining methods, namely, CNC milling and laser engraving. Attention is first directed to CNC milling. The CNC milling operation was accomplished with a HAAS VF-2 milling machine. The milling of PMMA and polycarbonate was accomplished using theoretical parameters acquired from a previous study [35]. Two primary operations were conducted, with drilling allowing for the creation of the outlet and end milling allowing for the creation of the inlets and microchannels. WD-40 was utilized as a coolant to prevent tool bit damage, given its brittle and thin nature. Drilling was conducted using a high-speed steel drill with a diameter of 2 mm. Tracing was then conducted with an HRC50 3-flute 1 mm diameter solid carbide tungsten steel end mill, with two passes conducted to prevent tool damage, as a single pass places heightened levels of stress on a 3-flute end mill. The machining parameters are presented in Table 1, with the average machining time for both PMMA- and polycarbonate-based microfluidic devices being 15 min. On the flip side, for borosilicate glass, boring

allowed for the creation of the outlet, and tracing operations allowed for the creation of the inlets and microchannels. Light mineral oil was utilized as a coolant, given its viscous properties. Boring and tracing operations were accomplished with diamond grinding bits. Ten passes were conducted to create a harmonious balance between microchannel quality and machining time and costs. Tables 3 and 4 present the milling parameters for PMMA and polycarbonate, and borosilicate glass, with an average machining time of 5 min and 1.25 h, respectively.

Attention will now be directed to the second fabrication technique: laser engraving. The laser engraving operation is accomplished with a BOSS LS-1416 and a lens with a 2-inch focal length. A significant dissimilarity from the design process of CNC milling is the absence of specific depth settings. Instead, different speeds, power levels, and pass quantities were experimented with. Calipers were utilized after a cross-section of the chip was made to ensure microchannel width and depth. This was also conducted with the outputs of the milling process to ensure that all results were of the design specification.

Multitudes of tests and adjustments were carried out to achieve the optimal parameters of laser-engraved PMMA microfluidic devices. RDWorks V8

was the software utilized to set the parameters and simulate the engraving processes. Two processes were conducted to achieve the results. First, the microchannels and inlets were scanned before the outlet hole was created through a cutting operation. Initial testing was carried out with microfluidic channels of larger radii in light of easier machinability from the high-speed qualities of laser engravers. A 2 mm radius served as the basis for the process through which parameter optimization was conducted. Laser speeds initially tested ranged from 100 mm/s and were increased in increments of 50 mm/s before acquiring the optimal speed of 250 mm/s, producing the best results. 2 passes were conducted to prevent overheating and leading to deformations within the microchannels. Once optimized, the creation of microfluidic devices with smaller radii, namely those of 1 mm and 1.5 mm radii, was conducted. Machine parameters for the laser engraving of PMMA slides are presented in Tables 5 and 6.

Table 3: Fabrication of microfluidic chips using PMMA and polycarbonate materials through the milling process.

Parameter	Value
Spindle Speed	8000 rpm
Drilling Surface Speed	50.2655 m/min
Tracing Surface Speed	25.1327 m/min
Drilling Plunge Feed Rate	145.531 mm/min
Cutting Feed Rate	305.1 mm/min
Hole Drill Time	10.03 s
Channel Trace Time	4:24 min
Number of Tracing Passes	2 passes

Table 4: Fabrication of microfluidic chips using borosilicate glass material through the milling process.

Parameter	Value
Spindle Speed	8000 rpm
Surface Speed	25.1327 m/min
Cutting Feed Rate	30-40 mm/min
Hole Drill Time	12:40 min/hole
Channel Trace Time	1:14:03 h
Number of Passes	10 passes

The engraving process of PMMA microfluidic devices only encountered minimal problems. On the contrary, the engraving process of borosilicate glass-based microfluidic devices underwent substantial challenges, including cracking. Various approaches were conducted, with the first being the submersion of the slide in cold, room temperature, and boiling water. Another approach conducted was pre-heating the glass to a temperature of 285 °C with a heating gun and validating the temperature with an infrared thermal imaging camera. Amongst these approaches, pre-

heating the glass yielded the best results. However, the heating process was conducted every two passes, as seen in Table 5, as the slides would significantly cool down past the two passes. The gradual cooldown after the 6th pass caused stemming cracks throughout the entire channel. Parameters were obtained from testing and previous studies that fabricate microchannels on glass [36].

Table 5: Fabrication of microfluidic chips using PMMA material through the laser engraving process.

Parameter	Value
Minimum Power	20% (14W)
Maximum Power	20% (14W)
Speed of Laser	250 mm/s
Number of Passes	2

Table 6: Fabrication of microfluidic chips using borosilicate glass material through laser engraving process.

Parameter	Value
Minimum Power	43% (30.1W)
Maximum Power	43% (30.1W)
Speed of Laser	250 mm/s
Number of Passes	10, heating every 2 passes

2.4 Conducting microfluidic chip post-processing techniques

Specification validation plays a crucial role in ensuring that all devices are up to manufacturing specifications. For each design, an extra device was manufactured to ensure that all devices possess the specified 1 mm microchannel width and depth. Here, the device was cut in half, and microchannel dimensions were acquired using a digital caliper with an accuracy of 0.0001 mm. Measurements were conducted in three sections: the start of the microchannels, the center channel, and just before the output. With this process, the researchers can ensure that all devices are up to specification and fluid mixing capabilities are not compromised.

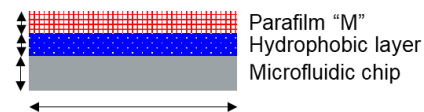


Figure 3: Layers of microfluidic device for testing.

Finally, a reliable sealing method plays a crucial role in ensuring that the microfluidic device functions as it should. However, before sealing the device, cleaning and treatments were conducted. Each device undergoes an ultrasonic cleaning process in water at

40 kHz for 10 minutes, ensuring that all unwanted debris is cleared off the microchannels and the surface. A layer of hydrophobic coating was added to allow for improved fluid flow. Parafilm “M” is a laboratory film that is considered a user-friendly material as it creates a quick and simple seal yet is cost-efficient [37]. To form a uniform seal, the film and microfluidic device were heated using a heat gun and pressed together. Figure 3 presents a visualization of the layers present.

To further support the reliability of the fabrication and preparation processes, Table 7 presents a summary of the experimental results for pre-treatment and fabrication conditions of various

materials and methods. Highlighted in this table are the tested pre-treatment strategies, outcomes, and optimal factors identified for CNC-milled PMMA, polycarbonate, and borosilicate glass, and laser-engraved borosilicate glass. Post-treatment through ultrasonic cleaning also allowed for cleaner microchannels and optimized results for all devices by preventing blockage. Through these findings, the significance of selecting materials and process-appropriate pre-treatment strategies for clean, reproducible, and high-quality microchannels is highlighted.

Table 7: Summary of pre- and post-treatments and optimal factors for microchannel fabrication.

Material and Method	Pre-Treatment	Outcome	Optimal Factors Identified
CNC-milled PMMA and Polycarbonate	WD-40 before milling	CNC coolant is too smelly and messy. WD-40 provided lubrication to prevent tool bit breakage.	Use WD-40 instead of coolant; Avoid CNC coolant
CNC-milled Borosilicate Glass	Light Mineral Oil before milling	Safe and effective, without risk of chemical contamination. CNC coolant is too smelly and messy.	Use oil instead of coolant; Avoid CNC coolant
Laser-engraved Borosilicate Glass	Pre-heating with a heat gun	Produced the best and most consistent results	Pre-heat the glass with a heat gun
Laser-engraved Borosilicate Glass	Hot water submersion	Worked once; Poor repeatability	Not recommended
Laser-engraved Borosilicate Glass	Cold water submersion	Did not work	Not recommended
Laser-engraved Borosilicate Glass	Hot and Cold water submersion	Did not work	Not recommended
All Chips	Ultrasonic cleaning	Effective cleaning method; Acid is not suitable for medical-grade devices	Use an ultrasonic cleaner; Avoid acid usage

2.5 Administering tests

In line with a previous study, food dye was utilized to test the mixing capabilities of the microchannels [18]. However, this experiment deviated from the method utilized through the sole focus of a 50:50 mixture of red and green dye rather than predetermined percentages. This process commenced through the creation of a standard 50% color mixture of red and green dye using accurate and precise measuring techniques, serving as a reference point for comparison. Photo analysis was then conducted to compare the colors of the outputs of each microfluidic device, looking into their deviations from the standard 50%. Do take note that using food dye is acceptable for proof-of-concept demonstrations due to its affordability, visibility, and ease of use. However, it may not fully capture the behavior of more complex fluids such as blood, reagents, or biological fluids, which differ in viscosity, surface tension, and

chemical composition. While this model provides a useful approximation, further testing with representative samples would be necessary to validate performance under actual operating conditions.

Next, microscopic views of the microchannels are also provided for qualitative analysis of each fabrication technique. The manual pump, as seen in Figure 4, was inspired by previous research, where the rig was designed for single-input microfluidic applications [19]. In this study, modifications were made to the manual pump to allow for two inlets into the mixing microchannels. To ensure simultaneous entry of both red and green dye into the microfluidic device, the flange was taped to the surrounding base to level the two syringes. Additionally, a slight engraving was made at the center of the base holding the 461g weight to ensure it was precisely centered. Thus, allowing both syringes to depress evenly. While there may be extremely slight delays at the microscopic level in one inlet due to manual control,

these are negligible for the purposes of this frugality-focused study. An automatic pump could minimize such delays, improving precision and repeatability. Nevertheless, the authors deem that the current setup is sufficient given the emphasis of the study on cost-effectiveness.

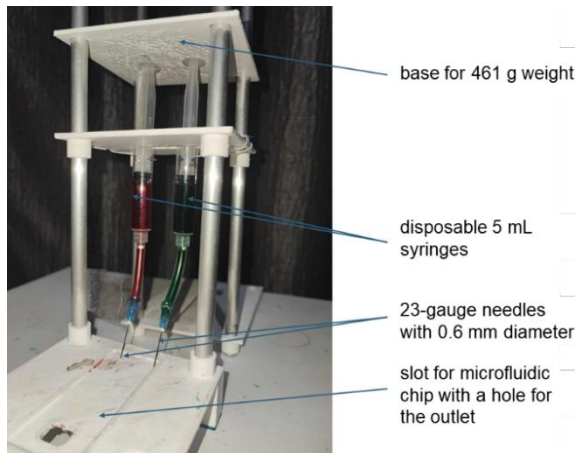


Figure 4: Actual setup of the manual pump.

Disposable syringes with a needle size of 23G or a needle length of 25 mm and an outlet diameter of 0.6 mm were used for the mixing of the fluids, where a constant mass of 461 g was placed on top to imitate a peristaltic pump. Analysis of the mixture was then conducted following the acquisition of a 5 mL output for each syringe, having a total output of 10 mL. The mass and output amount remained constant to maintain the same flow rates and output fluids, ensuring equal and comparable circumstances for all microfluidic devices.

When taking a photo of the mixture in the measuring cup, the camera captures a black or brown image, regardless of the actual color of the dye. As a solution, the paper was soaked in the mixture for 5 min and scanned through a color-calibrated printer (HP DeskJet Ink Advantage 2777). After, the scanned image was uploaded to an online program named Image Color Summarizer [38]. The program lists all the colors present in the photo and divides the amount of a certain color by the overall pixel amount of the photo, ensuring a fair and equal color analysis for all trials, regardless of inaccuracies in paper strip sizes.

3 Results and Discussion

3.1 Microscopic views of fabricated devices

The polycarbonate microfluidic devices that were fabricated through CNC milling would show fair consistency in the thickness of the milled grooves and paths, based on Figure 5(a). However, circular tool marks were seen due to the milling tool path, which may impact the surface smoothness of the material. The laser engraving process was not done for polycarbonate due to the fumes it would produce, which are toxic when inhaled. Microscopic views of CNC-milled and laser-engraved microfluidic devices in polycarbonate, PMMA, and borosilicate glass.

The fabricated PMMA microfluidic devices shown in CNC milling (Figure 5(b)) were able to produce well-defined edges with a smooth surface finish and consistent width throughout. It can be noted that minor edge irregularities were observed in the device. The devices produced using laser engraving (Figure 5(c)) would show a defined U-structure. However, the surface finish and the edges are rough, given the burning process. Parallel lines on the surface are present due to a back-and-forth motion during engraving.

For borosilicate glass-based microfluidic devices, microchannels produced through CNC milling would display smooth and defined edges with minimal cracks (Figure 5(d)). Tool bit marks would also be seen on both channels with different radii, indicating that the surface finish is slightly rough. The 1 mm microchannel fabricated using a CO₂ laser showed fewer cracks than the 1.5 mm microchannel (Figure 5(e)). The increased number of cracks may be caused by greater thermal stress induced by a larger radius during the fabrication process, leading to structural inconsistencies and damage. Possible modifications to the machining process to limit cracking include a lower cutting feed rate, a controlled annealing process, and laser-assisted machining. The inclusion of varying radii in Figure 5 is important for evaluating how each fabrication method performs across different channel sizes, as smaller radii are generally more difficult to manufacture but are critical for precise control in many microfluidic applications.

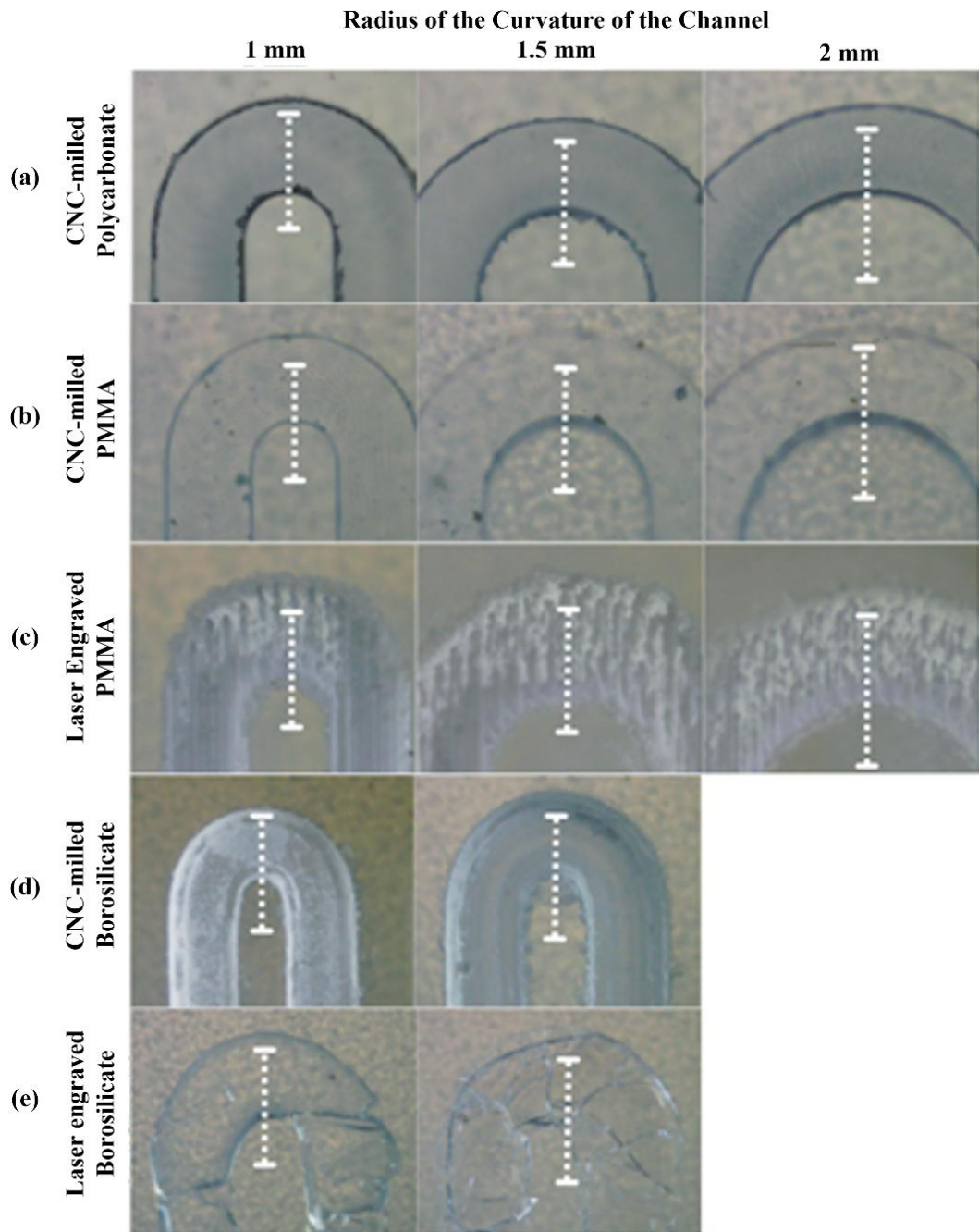


Figure 5: Microscopic views of the fabricated microfluidic chips: (a) CNC-milled polycarbonate, (b) CNC-milled PMMA, (c) laser-engraved PMMA, (d) CNC-milled borosilicate, and (e) laser-engraved borosilicate.

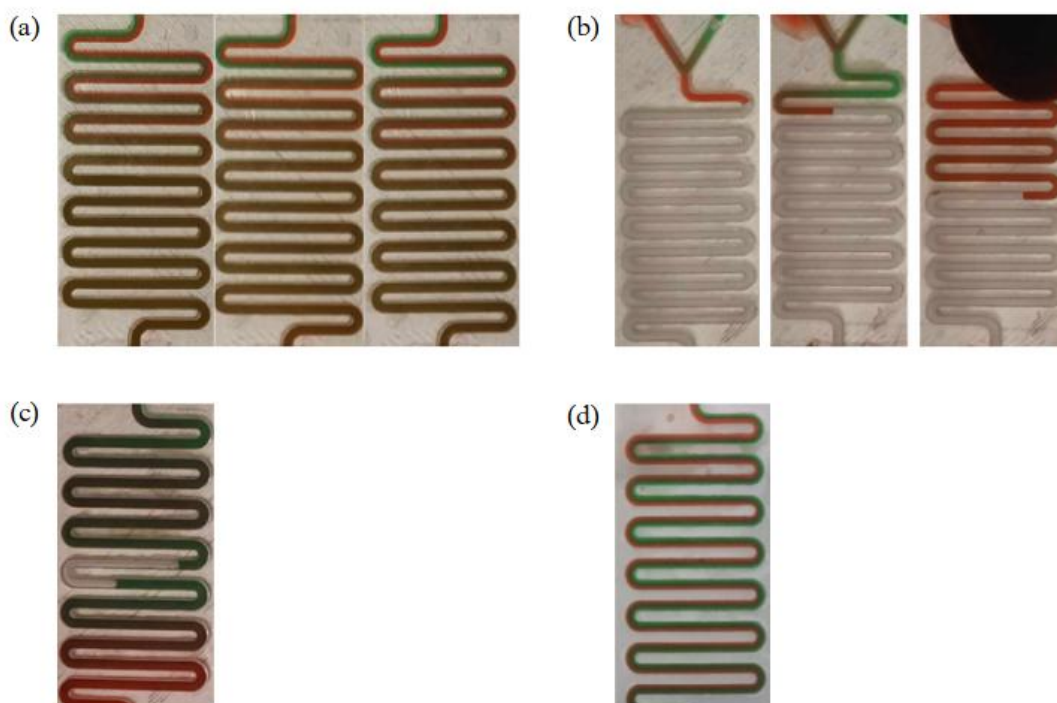


Figure 6: Comparison of CNC-milled and laser-engraved microfluidic chips: (a) CNC-PMMA testing, (b) laser-PMMA blockage points, (c) CNC-polycarbonate air bubble and congestion on V, (d) CNC-polycarbonate with increased mass/flow rate.

3.2 Color analysis of microfluidic channels

A mass of 461 g and a mixture output of 5 mL were defined as the constant testing parameters for this study. Amongst the various microfluidic chips tested, observations have proven that only the CNC-milled PMMA microfluidic devices have produced successful results with repeatability. Therefore, this type of microfluidic device was the only material in wherein color analysis was performed. Figure 6(a) shows where the red and green dyes similarly form a uniform shade after the 4th left curvature.

name	HEX	RGB
 236,220,227 abercrombie $\Delta E=2.1$	#F0DDE7	240 221 231

Figure 7: Output color in paper for control and trials.

For CNC-milled PMMA microfluidic devices, the output fluid appears to have a seemingly black or dark brown hue. Cameras also similarly capture these shades. Therefore, a sheet of paper was submerged

and soaked in the fluid for 5 min. Resultant of this, a hue with a mix of gray and pink shades was produced. Color-calibrated scans of the sheets of paper were conducted, and images were fed into an Image Color Summarizer. Figure 7 presents the hex code of the control and three trials, #F0DDE7. It is to be noted, however, that minor imperfections present in the paper were disregarded. The observed differences in the resultant colors highlight the varying degrees of mixing efficiency among the fabrication methods. A deviation from the reference hue may indicate incomplete mixing, material interference, or design-induced flow inconsistencies. In this study, a preliminary color of gray-pink hue was considered close to optimal, representing a balanced mix of red and green dyes. An optimal color output ideally exhibits minimal deviation from the reference standard. Establishing such a color range aids in quantifying mixing quality and serves as a benchmark for future tests

The successful yields of CNC-milled PMMA microfluidic devices have provided increased expectations for their laser-engraved counterparts.

However, for all three trials conducted, the laser-engraved devices experienced blockages at various points within the microchannels, as seen in Figure 6(b). Clogs within the system have been a result of this, and even with ultrasonic cleaning of all devices before testing, unwanted score marks and unwanted excess material on the microchannels are still present. This is primarily because laser engravers vaporize the material as it is an ablative process, where redeposited particles or debris of localized heating are likely to deform channel walls at microscopic levels.

As mentioned previously, polycarbonate-based microfluidic devices can only be created through CNC milling due to the potentially toxic fumes released from CO₂ laser engraving. Color analysis findings show that minor chips are presented in CNC-milled polycarbonate microfluidic devices compared to their PMMA counterparts. However, the prominent issue during the color analysis process lies within the “V” intersection of the microchannels before the mixing segments. In this section, congestion occurs, which causes air bubbles within the system or the mixture of the dye into the other inlet microchannel. As a result, the device clogs or air causes issues within the mixing microchannels in color analysis (Figure 6(c)).

A solution to the issue encountered lies within the mass to adjust the flow rates. An increase of approximately 200 g was applied, solving the issue and allowing the fluids to flow through the “V” intersection freely and eliminating the presence of air bubbles. But then, such a method has a limitation that lies in the number of attempts possible with the setup. Due to the increased levels of mass and flow rates, only a single attempt can be conducted before the pumps clog and stop functioning. The mixing capabilities are then hindered, with the dyes not mixing correctly due to the increased flow rate. To solve this, longer mixing microchannels are necessary (Figure 6(d)).

Serpentine microchannels with varied radius of curvature and fabrication methods were compared. Figure 6(a) shows a CNC-milled PMMA chip with 1mm curvature, presenting a relatively smooth flow but less efficient mixing due to reduced flow redirection, likely caused by the small radius of curvature. Figure 6(b) is a laser-engraved PMMA chip that shows flow irregularities due to fabrication-induced surface roughness (Figure 5(c)). The CNC-milled polycarbonate chip, while displaying a smooth surface area (Figure 5(a)), showcased bubble

entrapment for the smaller curvature (Figure 6(c)), while the microchannel with a larger curvature displayed increased mass and flow rate (Figure 6(d)).

Finally, there are borosilicate glass-based microfluidic devices. Testing was no longer conducted for both fabrication techniques, as cracks and impurities were observed in the microchannels. These fractures have been determined as limitations of the techniques conducted and have been observed to worsen as time passes. Table 8 presents the summary of test results, categorized by material, fabrication technique, and the three radii tested. For PMMA acrylic, both laser and CNC fabrication techniques successfully produced microchannels with all three radii. Due to the limitations mentioned previously, the laser engraving cannot be conducted with polycarbonate. Nevertheless, CNC-milled polycarbonate microfluidic devices still yield successful microchannels. Borosilicate glass then proved incompatible with both techniques, with neither method successfully fabricating channels of all radii. Although, through extended CNC machining time (up to 2 h) significantly less cracking was observed, this approach is impractical for a frugality-focused study, as operating a CNC machine for such durations is both time- and energy-intensive when producing just one microfluidic device. For laser engraving, water submersion and preheating were also tested. Preheating the glass to approximately 60 °C initially yielded results comparable to PMMA channels; however, once the borosilicate glass cooled down, the microfluidic channels began to crack after 20–30 min. Water submersion produced decent channels, but the vacuum inside the laser engraver introduced air pockets during the process, making the output inconsistent. In areas without adequate water coverage, the borosilicate chip still cracked, further reducing reliability.

Through these results, the limitations of the materials are highlighted along with an emphasis on selecting the appropriate fabrication techniques.

Table 8: Summary of test results based on qualitative and quantitative analysis.

Material	Fabrication Technique	1 mm Radius	1.5 mm Radius	2.0 mm Radius
PMMA Acrylic	Laser	✓	✓	✓
	CNC	✓	✓	✓
Polycarbonate	Laser	-	-	-
	CNC	✓	✓	✓
Borosilicate Glass	Laser	×	×	×
	CNC	×	✓	✓

Table 9: Comparison of the proposed study to the most related studies with CNC milling and CO₂ laser machining.

Material	Fabrication Technique	Pre-treatment	Channel Size (width × depth)	Surface Quality	Precision	Surface Roughness	Fabrication Time per Piece	Ref.
PMMA	CNC micromilling	None	200 μm × 50 μm	Smooth, crack-free	High	24–450 nm (optimum: 24 nm)	Not specified	[19]
K-PSFn214 glass	CO ₂ laser with preheating	250 °C Preheated	235 μm × 6 μm	Crack-free, minor bulging	Moderate	Not specified	Not specified	[36]
PMMA	CO ₂ laser machining	None	30–250 μm × 100–200 μm	Some roughness due to sublimation	Moderate	Before: 1.205 ± 0.243 nm After: 8.816 ± 2.653 nm	Not specified	[39]
PS	CO ₂ laser machining	None	50–300 μm × 100–250 μm	Very smooth surface due to melt-resolidify mechanisms	Moderate	Before: 3.319 ± 0.992 nm After: 1.327 ± 0.658 nm	Not specified	[39]
PMMA	CNC milling and CO ₂ laser machining	CNC milling: WD40	1 mm × 1 mm	CNC milling: smooth, crack-free; CO ₂ laser: rough	CNC milling: High; CO ₂ laser: moderate	Not part of the scope	CNC milling: 00:04:38 (~20 min. setup); CO ₂ laser: 00:01:17, (~1 min. setup)	Current Study
Polycarbonate	CNC milling	Light mineral oil	1 mm × 1 mm	smooth, minor chips	High	Not part of the scope	CNC milling: 00:04:38 (~20 min. setup);	Current Study
Borosilicate glass	CNC milling and CO ₂ laser with preheating	CNC milling: light mineral oil; CO ₂ laser: 285°C preheated	1 mm × 1 mm	CNC milling: smooth, minor cracks on edges; CO ₂ laser: rough, channels not formed	CNC milling: High; CO ₂ laser: low	Not part of the scope	CNC milling: 01:39:11 (~20 min. setup); CO ₂ laser: 00:01:17, (~1 min. setup)	Current Study

Table 9 presents a comparative analysis of the proposed study to other related studies utilizing CNC milling and CO₂ laser machining techniques. It was also presented that the capability of CNC micromilling in producing smooth, crack-free channels in PMMA with high precision and an optimal surface roughness of 24 nm is possible [19]. However, the study only encompasses relatively shallow depths of 50 μm and stringent control is necessitated to maintain surface integrity. It was also highlighted that the incorporation of pre-heating at 250 °C prior to laser machining K-PSFn214 glass, yielding crack-free surfaces with minor bulging [36]. However, only a narrow profile with a 235 μm width and a 6 μm depth was indicated. This suggests that further optimization may be needed.

CO₂ laser machining was investigated on PMMA and polystyrene without pre-treatment [39]. As a result, PMMA exhibited increased surface roughness due to sublimation effects, while polystyrene exhibited a significant reduction due to melt-resolidify mechanisms. Thus, it is presented that material properties can significantly influence surface outcomes.

The current study expounds on the findings through integrating pre-treatment, analyzing multiple materials, and evaluating surface quality before and after machining, with an aim to optimize fabrication parameters for improved dimension precision and

surface smoothness. Despite the increased fabrication time for CNC milling for this study, it can be observed that an improvement is present in the results. CNC milling consistently produced smoother surfaces and more defined channel profiles than laser engraving, particularly for PMMA and polycarbonate. This is due to the mechanical accuracy of the end mill, which avoids the heat-induced roughness seen in laser-engraved PMMA, where redeposition and localized melting degrade edge quality. In contrast, borosilicate glass, although chemically resistant, was more prone to cracking regardless of the fabrication technique. Laser engraving introduced thermal stress, while CNC milling caused mechanical stress—both contributing to the formation of cracks. Among all samples, CNC-milled PMMA demonstrated the most consistent and high-quality microchannels, balancing smooth surface finish, structural integrity, and manufacturing efficiency. These distinctions underscore the importance of selecting both the material and the corresponding fabrication method carefully to maximize microfluidic device performance.

In terms of scalability, each method presents its own set of pros and cons, dependent on the material being machined. CNC milling yields moderate to high quality but at a slower pace, making it a costly and time-consuming option for batch production. Each chip can be fabricated in approximately 5 min for a

polycarbonate or PMMA device, and 1.25 to 2 h for a borosilicate glass device. In contrast, laser engraving possesses the capability to fabricate devices at a higher rate but with low to moderate quality, making it suitable for low-cost batch production.

4 Conclusions

An in-depth comparison of the capabilities of CNC milling and CO₂ laser engraving as microfluidic chip fabrication techniques has been conducted. Four main objectives were determined: 1) develop a comparative analysis of CNC milling and CO₂ laser engraving for fabricating mixing microchannels in microfluidic devices, 2) propose an optimal fabrication strategy for combining precision, surface quality, and fluid dynamics, 3) evaluate borosilicate glass, PMMA, and polycarbonate as fabrication materials, and 4) identify a cost-effective method for producing high-performance microfluidic devices.

Qualitative and quantitative investigations present the exceptional qualities of CNC milling machines and PMMA in accuracy and repeatability. In addition, it combined excellent optical clarity, machinability, and cost-effectiveness. Polycarbonate and borosilicate glass yielded challenges concerning clarity and surface smoothness. On the flip side, the laser engraving of glass presented striking limitations through cracks emanating from thermal stress. PMMA devices were successfully created, but were not as exceptional in terms of surface smoothness and consistency as their milled counterparts. At the same time, polycarbonate chips cannot be engraved due to their toxic fume outputs. Thus, laser engraving may be better suited for simpler, low-cost designs where high precision is not critical.

Color analysis played a key role in validating results in this study. For future research, its integration into microfluidic systems offers strong potential for automated detection technologies, given their low sample and reagent use, cost-effectiveness, and real-time, in situ analysis capabilities. Color analysis can also be further enhanced through machine learning algorithms and image processing techniques to enable automated, high-throughput evaluation of mixing efficiency. In addition, adopting quantitative methods such as spectrophotometry and fluorescence intensity profiling would provide objective, high-resolution measurements of concentration gradients. These approaches are particularly valuable for assessing the effects of various microfluidic design features, such as channel elevation, serpentine paths, mixing ridges, or

3D geometries on flow dynamics. Combining advanced analysis methods with optimized designs could significantly improve the precision, repeatability, and scalability of microfluidic diagnostics.

Overall, the findings have emphasized the correlation between fabrication techniques and material properties. However, time and equipment constraints have hindered further optimizations, such as parameter fine-tuning. Machine limitations, such as lens focal length, have also presented limitations to this study. With this, future research can optimize fabrication parameters and investigate more materials to broaden the range of reliable yet cost-effective options for microfluidic device manufacturing. The integration of microfluidic device fabrication with other functionalities, such as valving, sensing, and real-time detection, can also be explored for more complex lab-on-a-chip systems. The establishment of guidelines for production-scale manufacturing can also play a vital role in commercial applications. Future designs may also delve into microchannel designs below 300 μm for a more realistic microfluidic condition, which maintaining manufacturability and integrity.

Acknowledgments

This study is supported by the Department of Science and Technology – Engineering Research and Development for Technology (DOST-ERDT) of the Philippines and the Office of the Vice President for Research and Innovation and the Science Foundation of De La Salle University, Manila.

Author Contributions

C.J.C.: conceptualization, investigation, methodology, writing an original draft, research design, data analysis; J.C.D.: conceptualization, investigation, methodology, writing an original draft, research design, data analysis, data curation, reviewing and editing; Z.N.: conceptualization, investigation, methodology, writing an original draft, research design, data analysis, data curation, reviewing and editing; B.S.U.: conceptualization, investigation, methodology, writing an original draft, research design, data analysis, data curation; R.J.T.A.: conceptualization, investigation, methodology, research design, data analysis, project administration; R.C.: conceptualization, investigation, reviewing and editing, methodology, research design, data analysis, writing—reviewing and editing, project administration. All authors have read and agreed to the published version of the manuscript.



Conflicts of Interest

The authors declare no conflict of interest.

References

- [1] B. Nasser, S. Akar, and E. Naseri, "Microchannels for microfluidic systems," in *Biomedical Applications of Microfluidic Devices*, New York: Academic Press, 2021, doi: 10.1016/b978-0-12-818791-3.00002-4.
- [2] I. Muzammil, A. I. Aqib, Q. Tanveer, S. Muzmmal, M. A. Naseer, and M. Tahir, "COVID-19 diagnosis—myths and protocols," *Data Science for COVID-19*, vol. 2, pp. 335–353, 2022, doi: 10.1016/b978-0-323-90769-9.00027-x.
- [3] L. Capretto, W. Cheng, M. Hill, and X. Zhang, "Micromixing within microfluidic devices," in *Topics in Current Chemistry*, 2011, pp. 27–68. doi: 10.1007/128_2011_150.
- [4] N. Convery & N. Gadegaard, "30 years of microfluidics," *Micro and Nano Engineering*, vol. 2, pp. 76–91, 2019, doi: 10.1016/j.mne.2019.01.003.
- [5] P. B. Kruk and J. A. Wippold, "PRIMDEX: Prototyping rapid innovation of microfluidics devices for experimentation," *SLAS Technology*, vol. 33, p. 100326, 2025, doi: 10.1016/j.slast.2025.100326.
- [6] N. Yasman, R. M. R. M. Fouzy, and M. Z. M. Zawawi, "Direct fabrication of glass microfluidic channel using CO₂ laser," *Materials Today: Proceedings*, vol. 97, pp. 52–60, 2024, doi: 10.1016/j.matpr.2023.11.048.
- [7] C. A. Leclerc et al., "Rapid design and prototyping of microfluidic chips via computer numerical control micromilling and anisotropic shrinking of stressed polystyrene sheets," *Microfluidics and Nanofluidics*, vol. 25, no. 2, 2021, doi: 10.1007/s10404-020-02414-7.
- [8] S. M. Scott and Z. Ali, "Fabrication methods for microfluidic devices: An overview," *Micromachines*, vol. 12, no. 3, 2021, doi: 10.3390/mi12030319.
- [9] N. Shanehband and S. M. Naghib, "Recent advances in nano/microfluidics-based cell isolation techniques for cancer diagnosis and treatments," *Biochimie*, vol. 220, pp. 122–143, 2024, doi: 10.1016/j.biochi.2024.01.001.
- [10] T. Zhang et al., "Passive microfluidic devices for cell separation," *Biotechnology Advances*, vol. 71, p. 108317, 2024, doi: 10.1016/j.biotechadv.2024.108317.
- [11] P. Cui and S. Wang, "Application of microfluidic chip technology in pharmaceutical analysis: A review," *Journal of Pharmaceutical Analysis*, vol. 9, no. 4, pp. 238–247, 2019, doi: 10.1016/j.jpha.2018.12.001.
- [12] A. Saikia, R. Newar, S. Das, A. Singh, D. J. Deuri, and A. Baruah, "Scopes and challenges of microfluidic technology for nanoparticle synthesis, photocatalysis and sensor applications: A comprehensive review," *Chemical Engineering Research and Design*, vol. 193, pp. 516–539, 2023, doi: 10.1016/j.cherd.2023.03.049.
- [13] K. R. J. Pou, V. Raghavan, and M. Packirisamy, "Microfluidics in smart packaging of foods," *Food Research International*, vol. 161, p. 111873, 2022, doi: 10.1016/j.foodres.2022.111873.
- [14] D. Yang, M. N. Kashani, and C. Priest, "Pilot-scale microfluidic solvent extraction of high-value metals," *Minerals Engineering*, vol. 182, p. 107536, May 2022, doi: 10.1016/j.mineng.2022.107536.
- [15] M. Akbari and A. Seyfoori, "Microfluidic device with integrated magnets for biomarker detection and manipulation." Espacenet. Accessed: May 13, 2025. [Online.] Available: <https://worldwide.espacenet.com/patent/search/family/089770086/publication/US2024042443A1?q=microfluidic%20device%20with%20integrated%20magnets%20for%20biomarker>
- [16] D. Appleyard et al. "Microfluidic system and method with focused energy apparatus." Google Patents. Accessed: May 13, 2025. [Online.] Available: <https://patentimages.storage.googleapis.com/e5/1c/b0/f912cdfb88927d/AU2023270339A1.pdf>
- [17] Y. S. Zhang and X. Kuang, "Double networked 3D-printed biomaterials." Espacenet. Accessed: May 13, 2025. [Online.] Available: <https://worldwide.espacenet.com/patent/search?q=pn%3DEP4561645A2>
- [18] Z. Akbari, M. A. Raoufi, S. Mirjalali, and B. Aghajanloo, "A review on inertial microfluidic fabrication methods," *Biomicrofluidics*, vol. 17, no. 5, 2023, doi: 10.1063/5.0163970.
- [19] M. S. Rahim and A. A. Ehsan, "Micro milling process for the rapid prototyping of microfluidic devices," in *Advances in Microfluidics and Nanofluids*, S. M. S. Murshed, Ed., London, UK: IntechOpen, 2021, doi: 10.5772/intechopen.96723.
- [20] H. van Heeren et al. "Protocols for leakage testing." White paper. Accessed: May 13, 2025. [Online.] Available: <https://chipsproject.eu/wp->

- content/uploads/2022/07/CHIPS-Protocols-for-leakage-testing.pdf
- [21] L. Ding et al., "A modular 3D printed microfluidic system: A potential solution for continuous cell harvesting in large-scale bioprocessing," *Bioresources and Bioprocessing*, vol. 9, no. 1, 2022, doi: 10.1186/s40643-022-00550-2.
- [22] O. R. Chanu, A. Kapoor, and V. Karthik, "Digital image analysis for microfluidic paper based pH sensor platform," *Materials Today: Proceedings*, vol. 40, no. 1, pp. S64–S68, 2021, doi: 10.1016/j.matpr.2020.03.503.
- [23] M. Golozar, W. K. Chu, L. D. Casto, J. McCauley, A. L. Butterworth, and R. A. Mathies, "Fabrication of high-quality glass microfluidic devices for bioanalytical and space flight applications," *MethodsX*, vol. 7, p. 101043, 2020, doi: 10.1016/j.mex.2020.101043.
- [24] Y. Chen, L. Zhang, and G. Chen, "Fabrication, modification, and application of poly(methyl methacrylate) microfluidic chips," *Electrophoresis*, vol. 29, no. 9, pp. 1801–1814, 2008, doi: 10.1002/elps.200700552.
- [25] P. Jankowski and P. Garstecki, "Stable hydrophilic surface of polycarbonate," *Sensors and Actuators B Chemical*, vol. 226, pp. 151–155, Nov. 2015, doi: 10.1016/j.snb.2015.11.100.
- [26] W. Wu, Q. Ouyang, L. He, and Q. Huang, "Optical and thermal properties of polymethyl methacrylate (PMMA) bearing phenyl and adamantyl substituents," *Colloids and Surfaces a Physicochemical and Engineering Aspects*, vol. 653, p. 130018, Aug. 2022, doi: 10.1016/j.colsurfa.2022.130018.
- [27] N. Kiomarsipour, A. Eshaghi, M. Ramazani, H. Zabolian, and M. Abbasi-Firouzjah, "Investigation of upward speed and thickness effects on optical and mechanical properties of hard transparent thin films deposited on polycarbonate substrate," *Progress in Organic Coatings*, vol. 177, p. 107405, Jan. 2023, doi: 10.1016/j.porgcoat.2023.107405.
- [28] S. Kumar, K. Singh, and D. Kumar, "SiO₂/B₂O₃ glass formers effect on transparency and mechanical properties of soda-lime borosilicate glasses for automobile applications," *Journal of Non-Crystalline Solids*, vol. 618, p. 122530, Aug. 2023, doi: 10.1016/j.jnoncrysol.2023.122530.
- [29] Y. Arcot, G. L. Samuel, and L. Kong, "Manufacturability and surface characterisation of polymeric microfluidic devices for biomedical applications," *The International Journal of Advanced Manufacturing Technology*, vol. 121, no. 5–6, pp. 3093–3110, Jun. 2022, doi: 10.1007/s00170-022-09505-5.
- [30] H. J. Imran, K. A. Hubeatir, and M. M. Al-Khafaji, "CO₂ Laser Micro-Engraving of PMMA complemented by Taguchi and ANOVA methods," *Journal of Physics Conference Series*, vol. 1795, no. 1, p. 012062, Mar. 2021, doi: 10.1088/1742-6596/1795/1/012062.
- [31] K. Vipindas and J. Mathew, "Machining of borosilicate glass using Micro-End milling," in *All India Manufacturing Technology, Design and Research Conference (AIMTDR)*, 2019, pp. 189–200, doi: 10.1007/978-981-32-9425-7_16.
- [32] Central Drug House (P) Ltd. "Polymethyl methacrylate; CAS No. 9011-14-7." Cdhfinechemical. Accessed: May 13, 2025. [Online.] Available: https://www.cdhfinechemical.com/images/product/msds/37_1325290147_PO_LYMETHYLMETHACRYLATECASNO9011-14-7MSDS.pdf
- [33] Aladdin Scientific Corporation, "Polycarbonate," CAS No. 25037-45-0, Feb. 6, 2024.
- [34] Sigma-Aldrich, "Borosilicate glass," CAS No. 308062-88-6, Aug. 25, 2020.
- [35] M. P. Jahan, J. Ma, C. D. Hanson, and G. K. Arbuckle, "Tool wear and resulting surface finish during micro slot milling of polycarbonates using uncoated and coated carbide tools," *Proceedings of the Institution of Mechanical Engineers, Part B: Journal of Engineering Manufacture*, vol. 234, no. 1–2, pp. 52–65, Jul. 2019, doi: 10.1177/0954405419862479.
- [36] N. Yasman, R. M. R. M. Fouzy, and M. Z. M. Zawawi, "Direct fabrication of glass microfluidic channel using CO₂ laser," *Materials Today Proceedings*, vol. 97, pp. 52–60, Nov. 2023, doi: 10.1016/j.matpr.2023.11.048.
- [37] A. K. Fajrial, A. Vega, G. Shakya, and X. Ding, "A frugal microfluidic pump," *Lab on a Chip*, vol. 21, no. 24, pp. 4772–4778, Jan. 2021, doi: 10.1039/d1lc00691f.
- [38] M. Krzywinski. "Image Color Summarizer - RGB and HSV Image Statistics." Bcgsc.ca. Accessed: May 13, 2025. [Online.] Available: <https://mk.bcgsc.ca/color-summarizer/?home>
- [39] Bilican and M. T. Guler, "Assessment of PMMA and polystyrene based microfluidic chips fabricated using CO₂ laser machining," *Applied Surface Science*, vol. 534, p. 147642, Aug. 2020, doi: 10.1016/j.apsusc.2020.147642.